


Optimizing 3D-Printed Auxetic Structures for Tensile Performance: Taguchi Method Application on Cell Size and Shape Orientation

Fatih Pehlivan^{1,*} 

¹Karabük University, Faculty of Engineering, Karabük, Turkey

ARTICLE INFORMATION

Received: 30.10.2024

Accepted: 12.12.2024

Keywords:

Auxetic structures
Stereolithography
Additive
manufacturing
Taguchi method
Mechanical properties
Optimization

ABSTRACT

Auxetic structures are characterized by their unique mechanical property of exhibiting a negative Poisson's ratio, which means they expand laterally when stretched and contract laterally when compressed, contrary to conventional materials. This distinctive behavior enables auxetic materials to possess enhanced mechanical properties such as improved energy absorption, shear resistance, and indentation resistance. This study is of special novelty as it is one of the few investigations examining the effect and optimization of shape orientation and cell size on tensile mechanical properties. For this reason, a total of nine different specimens were produced using three different cell sizes (3 mm, 2 mm, 1.5 mm) and three different shape orientations (0°, 45°, 90°) using a masked stereolithography (MSLA) printer, and their tension mechanical properties were investigated. The best cell size and shape orientation were determined by Taguchi's maximum signal-to-noise ratio (S/N) analysis, and the data was analyzed with the Analysis of Variance (ANOVA) test. Specifically, a cell size of 1.5 mm and a shape orientation of 90° delivered the best performance, with a maximum fracture force of 348.44 N and energy absorption of 224.91 J. This research contributes to optimizing 3D printing for improved mechanical performance and to the field of additive manufacturing.

Çekme Performansı için 3B Baskılı Auxetic Yapıların Optimizasyonu: Hücre Boyutu ve Şekil Yönelimi Üzerine Taguchi Yönteminin Uygulaması

MAKALE BİLGİSİ

Alınma: 30.10.2024

Kabul: 12.12.2024

Anahtar Kelimeler:

Auxetic yapılar
Stereolitografi
Eklemeli imalat
Taguchi yöntemi
Mekanik özellikler
Optimizasyon

ÖZET

Auxetic yapılar, negatif Poisson oranı sergileyen benzersiz mekanik özellikleriyle karakterize edilir; bu, geleneksel malzemelerin aksine, gerildiklerinde yanıl olarak genişledikleri ve sıkıştırıldıklarında yanıl olarak büzüldükleri anlamına gelir. Bu ayırt edici davranış, auxetic malzemelerin gelişmiş enerji emilimi, kayma direnci ve çentik direnci gibi gelişmiş mekanik özelliklere sahip olmasını sağlar. Bu çalışma, şekil yöneliminin ve hücre boyutunun çekme mekanik özellikleri üzerindeki etkisini ve optimizasyonunu inceleyen az sayıda araştırma birisi olması nedeniyle özel bir yenilik taşımaktadır. Bu nedenle, maskeli stereolitografi (MSLA) yazıcısı kullanılarak üç farklı hücre boyutu (3 mm, 2 mm, 1.5 mm) ve üç farklı şekil oryantasyonu (0°, 45°, 90°) kullanılarak toplam dokuz farklı numune üretilmiş ve bunların gerilme mekanik özellikleri incelenmiştir. En iyi hücre boyutu ve şekil yönelimi Taguchi'nin maksimum sinyal-gürültü oranı (S/N) analizi ile belirlenmiş ve veriler Varyans Analizi (ANOVA) testi ile analiz edilmiştir. Özellikle, 1.5 mm'lik bir hücre boyutu ve 90°'lik bir şekil yöneliminin, 348.44 N'lik maksimum kırılma kuvveti ve 224.91 J'lik enerji emilimi ile en iyi performansı sağladığı bulunmuştur. Bu araştırma, gelişmiş mekanik performans için 3B baskının optimizasyonuna ve eklemeli imalat alanına katkıda bulunmaktadır.

1. INTRODUCTION (GİRİŞ)

Auxetic structures constitute an attractive category of materials defined by their outstanding mechanical properties, especially the negative Poisson's ratio, providing lateral expansion upon tensile deformation. This unusual behavior significantly contrasts with ordinary materials, which

*Corresponding author, e-mail: fatihpehlivan@karabuk.edu.tr

To cite this article: F. Pehlivan, Optimizing 3D-Printed Auxetic Structures for Tensile Performance: Taguchi Method Application on Cell Size and Shape Orientation, Manufacturing Technologies and Applications, 5(3), 287-297, 2024.

<https://doi.org/10.52795/mateca.1576416>, This paper is licensed under a CC BY-NC 4.0

contract laterally under tensile stress. The investigation of auxetic structures has attracted considerable attention in recent years, propelled by their potential uses in diverse domains, such as biomedical engineering, aircraft, lightweight structural elements, and protective equipment. The capacity of these materials to efficiently absorb energy and their superior mechanical properties, including increased shear and indentation resistance, make them especially attractive for new design solutions in engineering and materials science [1,2]. Due to their potential applications in medicinal devices, protective gear, and aerospace components that require energy absorption and impact resistance, auxetic materials have gained popularity [3]. Auxetic materials are ideal for sporting equipment because they can dissipate energy and adapt to body movements, thus improving comfort and safety [4]. Auxetic structures also have the potential to enhance the design of implants and prostheses in biomedical applications by mimicking the mechanical behavior of biological tissues [5]. In addition, their distinctive deformation mechanisms contributed to research into their potential applications in crashworthiness and protective gear, where energy absorption is essential [6,7].

The development of additive manufacturing has transformed the fabrication of auxetic structures. This novel method facilitates the production of intricate geometry that conventional manufacturing techniques find challenging to accomplish. Additive manufacturing methods, especially 3D printing, facilitate precise regulation of material characteristics and geometric configurations, thus improving the functionality of auxetic structures [8–10]. Research has shown the effective 3D printing of polymer-based auxetic structures by methods like Masked Stereolithography Apparatus (MSLA), enabling significant design flexibility and facilitating mass production [11,12]. The integration of new materials, including carbon fiber-reinforced polymers, into the additive printing process has significantly boosted the mechanical properties of auxetic structures, leading to improved strength and durability [13]. Furthermore, the incorporation of soft materials in 3D printing has facilitated the development of auxetic structures with enhanced energy absorption properties, rendering them suitable for impact protection applications [14].

The cell size and shape orientation of auxetic structures play a crucial role in influencing their mechanical characteristics. Auxetic materials demonstrate distinctive deformation characteristics significantly affected by the geometric design of their unit cells. The configuration of these cells, related to their dimensions and alignment, may greatly impact the structural integrity, energy absorption capability, and rigidity of the auxetic structures [15,16]. Smaller unit cells can improve the mechanical performance of auxetic materials by increasing the surface area and facilitating more complex designs that maximize load distribution during deformation [15,16]. The orientation of cells in an auxetic structure also influences its mechanical properties. Various orientations can result in differences in stiffness and energy absorption properties, as the load-bearing capacities of the cells change according to their alignment [17]. Studies demonstrate that the configuration of cells can affect the material's overall response to stress, with specific arrangements yielding enhanced performance in applications like impact resistance and cushioning [14,18].

The enhancement of tensile mechanical properties in 3D printing has emerged as a key area of research, especially with the rising need for high-performance materials in many industries. The Taguchi technique is a popular statistical tool used for experimental design and optimization. This method is an effective tool for examining the effect of multiple factors and evaluates the level of improvement of target performance through S/N ratio analysis. It enables researchers to systematically assess the impact of various process factors on the mechanical properties of 3D printed components, which enables the identification of optimal conditions that improve tensile strength and elongation [19,20]. The Taguchi approach employs orthogonal arrays to reduce the number of experiments necessary while enhancing the information obtained, rendering it both economical and efficient [21]. This method is particularly beneficial in additive manufacturing, where parameters such as layer thickness, infill density, and printing speed significantly affect the tensile strength and overall performance of printed components [22,23]. By employing the Taguchi method, researchers can identify optimal combinations of these parameters, leading to enhanced mechanical properties while minimizing the number of experimental trials required [24,25]. In

addition to process parameters, the geometric characteristics of the printed structures, specifically cell size and shape orientation, play a pivotal role in determining the mechanical behavior of auxetic materials. Auxetic structures are notably flexible to the configuration and dimensions of their unit cells. Research indicates that variations in cell size might result in substantial variances in tensile strength and energy absorption capability [16].

This investigation is particularly significant for its originality, as it is one of the few to investigate the impact and optimization of shape orientation and cell size on the tensile mechanical properties of re-entrant auxetic structures, which are often the subject of research [26,27] due to their simplicity, mechanical performance and versatility. Consequently, 9 distinct specimens were fabricated utilizing 3 different cell sizes (3 mm, 2 mm, 1.5 mm) and 3 different shape orientations (0° , 45° , and 90°) through the MSLA technique using the same ABS material. The Taguchi method was utilized to optimize the maximum fracture force and energy absorption by determining the optimum combination of cell size and shape orientation. The results were additionally examined utilizing analysis of variance (ANOVA). This study aimed to address a gap in the literature by investigating the tensile properties of re-entrant auxetic structures printed using MSLA 3D printing.

2. MATERIAL AND METHOD (MATERYAL VE YÖNTEM)

2.1. Design of Re-Entrant Auxetic Structure

The ASTM D638-14 standards employed a dog-bone-shaped specimen with appropriately placed re-entrant auxetic structures within the testing section for the tension test. Specimen dimensions were obtained from a Type IV model, as illustrated in Figure 1, and Solidworks software was employed to generate the computer-aided design (CAD) shape.

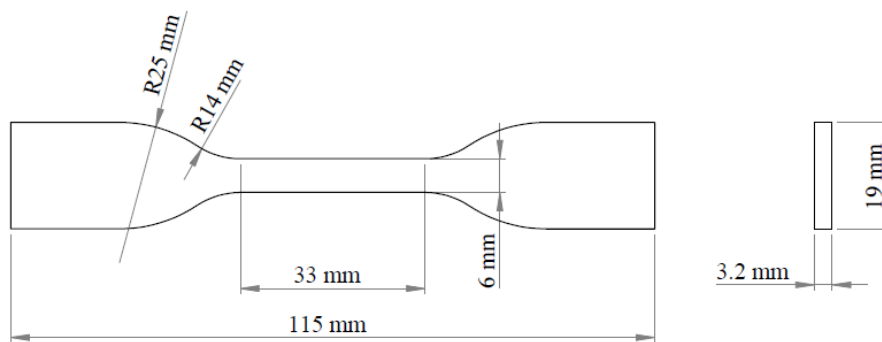


Figure 1. The geometry of the experimental specimen, based on ASTM D638-14 standards.

The tensile test specimens were 0.6 mm thick (t) and were designed to fit 2, 3 and 4 of the re-entrant auxetic unit cells shown in Figure 2 in the 0° shape orientation within the 6 mm width of the test zone. Therefore, cell sizes (h_a) of 3 mm, 2 mm, 1.5 mm were determined within minimum and maximum value constraints, taking into account design objectives and manufacturability. Shape orientation values (0° , 45° , 90°) were also chosen within the maximum, minimum and average values.

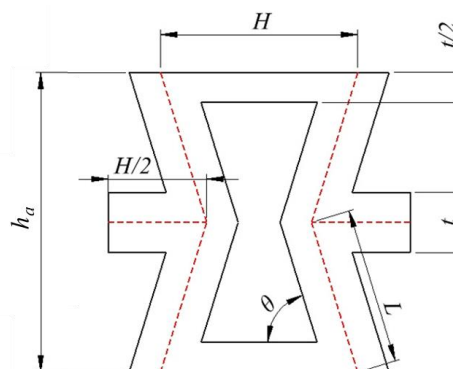


Figure 2. The unit cell of the auxetic structure (Auxetic yapının birim hücresi)

These cells were then rotated by 45° and 90° and placed in the test area and then the shape orientations of the re-entrant auxetic structures were designed using SolidWorks software as shown in Figure 3, resulting in three distinct plans (0° , 45° , 90°).

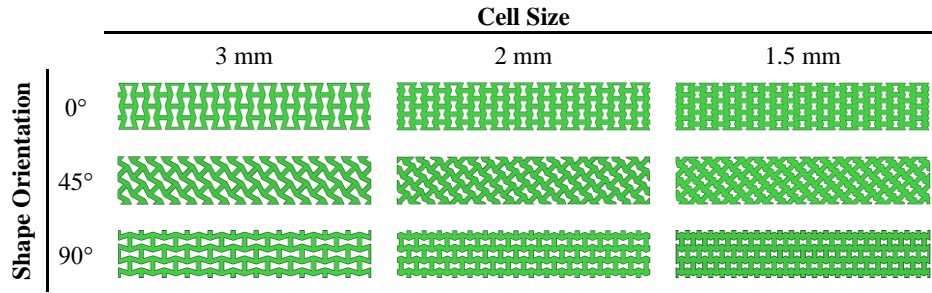


Figure 3. Designs of the test areas of the tensile specimens.

2.2. Printing of The Test Specimens (Test Numunelerinin Basılması)

Following the re-entrant auxetic structures were saved as STL files, they were imported into the Photon Workshop slicing software developed by Anycubic to establish the print settings and the position of the specimens on the build plate. The re-entrant auxetic specimens were fabricated utilizing acrylonitrile butadiene styrene (ABS)-like resin and the Anycubic Photon Mono M3 MSLA 3D printer. The study employed the suggested print settings for ABS resin specially 0.05 mm layer thickness and 4 s exposure time. Figure 4 displays the images of the fabricated specimens in the test area.

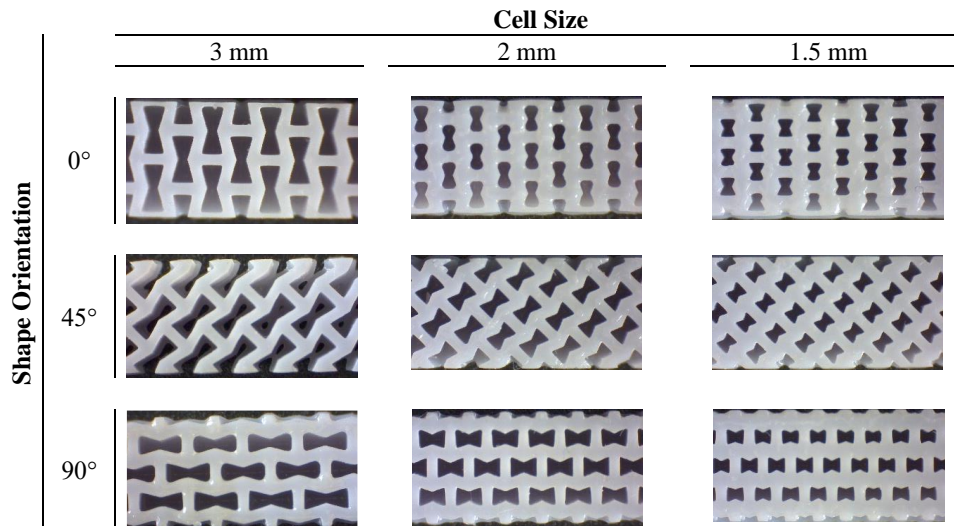


Figure 4. Images of the test areas of the manufactured tensile specimens (Üretilen çekme numunelerinin test alanlarının görüntüleri)

Employing criteria from the design of experiment (DOE) method, 9 distinct specimens, as shown in Figure 5, were produced, with 3 specimens provided for each sample to reduce the impact of random error sources and variability. The Anycubic wash & cure 2.0 equipment was employed to conduct a final curing procedure that lasted 40 minutes in order to improve the mechanical properties of the produced samples.

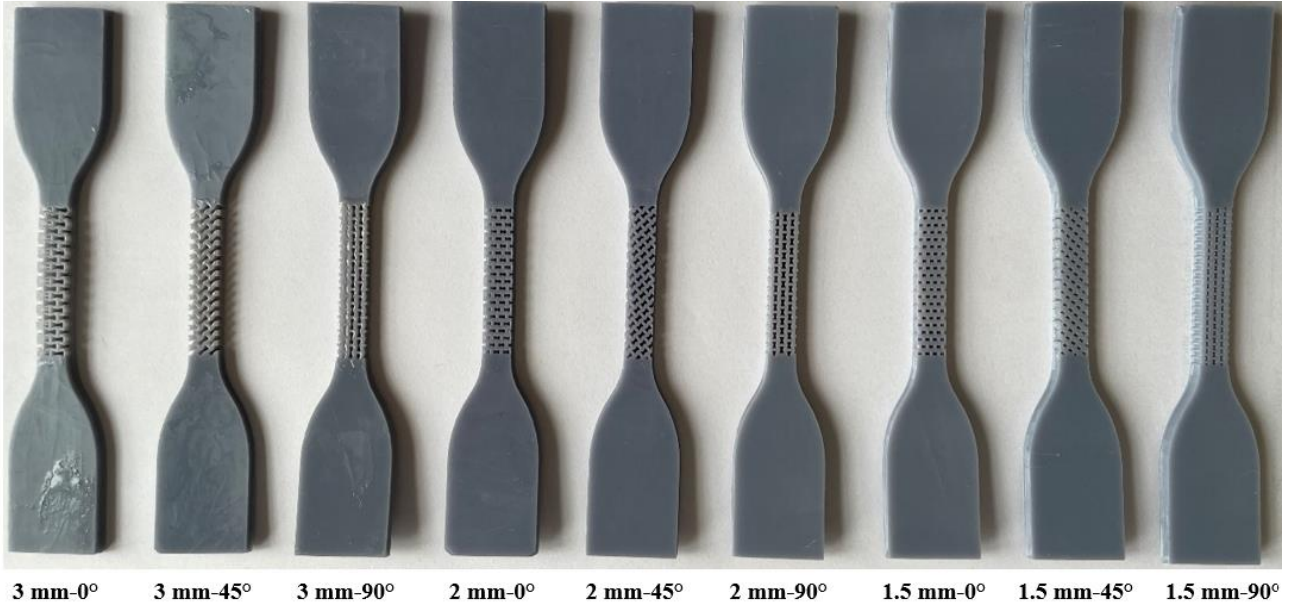


Figure 5. A manufactured sample of tensile specimens (Çekme numunelerinin üretilmiş bir örneği)

2.3. Tension Test (Çekme Testi)

The tensile test was conducted using a Shimadzu Autograph universal testing machine, following the guidelines outlined in ASTM standards D638. The displacement rate was recorded at 5 mm/min and the specimens were subjected to a progressively increasing load until failure occurred. The load and displacement data were recorded in the experimental setup and later used to determine the mechanical properties. A specimen of the tensile test is shown in Figure 6.



Figure 6. A specimen of the tensile test (Çekme deneyinden bir numune)

2.4. Optimization (Optimizasyon)

The Taguchi method provides a statistically robust approach, enabling researchers to identify optimal operating conditions while minimizing the number of experiments, thereby reducing both the time and costs associated with experimental processes. An advantage of the Taguchi method is its use of orthogonal arrays for experimental design, which simplifies the planning process while also acknowledging the limitations in controlling all variables that contribute to variability, often referred to as noise factors. This research employed a full factorial design with two factors, each at three levels, to systematically and comprehensively examine the potential interactions and effects of these factors on a specified response or output utilizing the Taguchi method. Factors believed to influence force at break and energy absorption include the dimensions and orientations of the re-

entrant auxetic structures. Table 1 illustrates the factors considered along with their respective levels.

Table 1. Taguchi L9 orthogonal array (Taguchi L9 ortogonal dizi)

Factors	Levels		
Cell size	3 mm	2 mm	1.5 mm
Shape orientation	0°	45°	90°

The study employed Taguchi's L9 orthogonal array for experimental design optimization. Minitab's L9 Taguchi orthogonal array was employed to create main effects plots for the signal-to-noise (S/N) ratio related to mechanical properties. Given that the objective of this study was to enhance tensile strength, specifically the force at break and energy absorption, the "larger is better" criterion was selected using Equation (1).

$$S/N = -10 \log_{10} \left[\frac{1}{n} \sum_{i=1}^n \frac{1}{y_i^2} \right] \quad (1)$$

3. RESULTS AND DISCUSSION (SONUÇLAR VE TARTIŞMA)

This section presents and evaluates the mechanical response derived from tensile tests of three cell sized re-entrant auxetic structures with different shape orientations. Tensile tests were used to determine the force at break and absorbed energy. Each measurement was averaged over the repeated specimens, and the mean findings with standard deviations are shown in Table 2. Force at break peaks at 348.44 N for run 9 and drop to 57.81 N for run 2. Similarly, run 9 and run 2 had the highest (224.91×10^{-3} J) and lowest absorbed energy (17.06×10^{-3} J), respectively. According to these findings, the optimal cell size and shape orientation for both force at break and absorbed energy are 1.5 mm and 90°, respectively. In order to enhance the clarity of these findings, descriptive statistics are presented in Table 2. This table presents the minimum and maximum values as well as the mean values and standard deviations for each run.

Table 2. Results of the tensile test (Çekme testi sonuçları)

Run	Cell size	Shape orientation	Force \pm SD (N)	Energy \pm SD ($\times 10^{-3}$ J)
1	3 mm	0°	96.87 \pm 5.62	53.01 \pm 3.21
2	3 mm	45°	57.81 \pm 3.88	17.06 \pm 1.54
3	3 mm	90°	176.56 \pm 16.05	73.84 \pm 4.27
4	2 mm	0°	142.19 \pm 14.31	57.72 \pm 3.98
5	2 mm	45°	103.12 \pm 8.09	48.62 \pm 3.60
6	2 mm	90°	325.00 \pm 27.54	181.92 \pm 19.97
7	1.5 mm	0°	170.31 \pm 14.33	71.26 \pm 4.62
8	1.5 mm	45°	137.50 \pm 8.46	59.70 \pm 3.74
9	1.5 mm	90°	348.44 \pm 31.18	224.91 \pm 10.98

Figure 7 shows the force-displacement curves for tensile tests on specimens containing re-entrant auxetic cells oriented at 0°, 45°, and 90°, with different cell sizes in the test area: 3 mm, 2 mm, and 1.5 mm. In the 3 mm cell size configuration, the 90° orientation shows the highest force resistance. The 0° and 45° orientations show lower force responses, while the 45° orientation shows a failure of about 0.6 mm elongation. In the 2 mm cell size configuration, the 90° orientation continues to demonstrate the highest force at break. The 0° and 45° orientations follow similar trends as observed in the 3 mm cell size case, with gradual force increases up to the failure point. The overall force capacity is higher than that of the 3 mm cell size configuration, suggesting that increasing the number of cells enhances the specimen's structural strength. The 1.5 mm cell size configuration maintains this pattern, with the 90° orientation again showing the greatest force resistance and achieving a peak force of around 350 N. This indicates that decreasing the cell size results in a

stronger and stiffer structure. The 0° and 45° orientations exhibit similar behavior, with slightly higher force values prior to yielding compared to previous configurations.

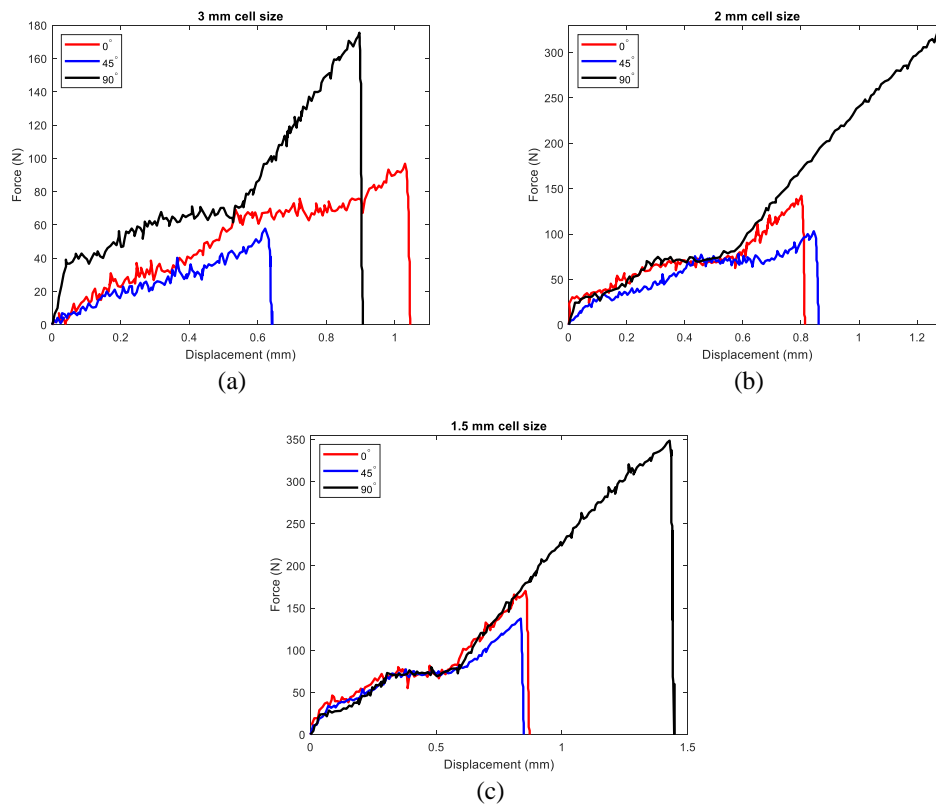


Figure 7. Force-displacement curves of tensile specimens containing different cell sizes in the test area (a) 3 mm, (b) 2 mm and (c) 1.5 mm.

Figure 8 presents the force-displacement curves from tensile tests conducted on specimens with different shape orientations: 0° , 45° , and 90° . Each graph compares three configurations with cell sizes 3 mm, 2 mm and 1.5 mm, respectively. In the 0° shape orientation, the specimen with a 1.5 mm cell size exhibits the highest force value, followed by the 2 mm and 3 mm cell size configurations. This observation is supported by the literature, which suggests that specimens with smaller cell sizes are able to withstand larger forces before failure [28]. The 1.5 mm cell size configuration shows a steep increase in force, indicating stronger material response, while the 3 mm cell size configuration demonstrates a comparatively lower force capacity. For the 45° shape orientation, the force capacity decreases across all configurations compared to the 0° shape orientation. However, the 1.5 mm cell size configuration still withstands the highest force. The displacement at failure is similar among configurations but slightly reduced relative to the 0° shape orientation. In the 90° shape orientation, the specimen with a 1.5 mm cell size once again demonstrates the highest force, while the 3 mm cell size specimen shows the lowest. The displacement patterns resemble those in the 0° shape orientation, suggesting that the material maintains its strength in the 90° shape orientation nearly as effectively as in the 0° orientation.

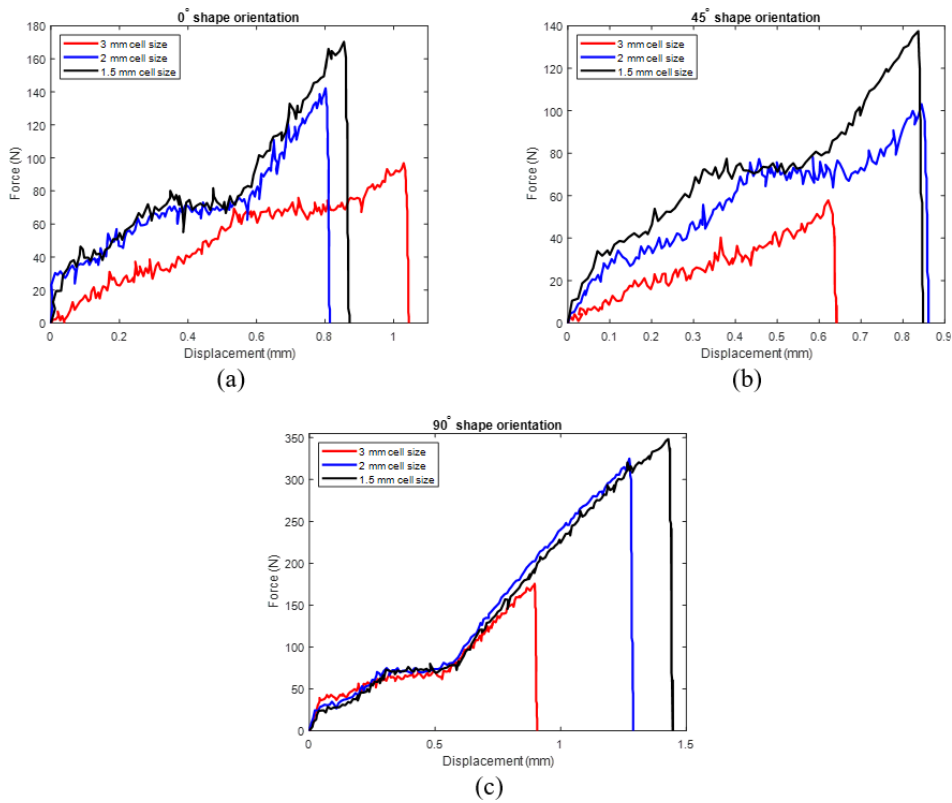


Figure 8. Force-displacement curves of tensile specimens containing different shape orientations in the test area (a) 0°, (b) 45° and (c) 90°.

Table 3 shows that the influence of shape orientation of the re-entrant auxetic structure on force at break and absorbed energy is 70.88% and 64.66%, respectively which was significantly higher than cell size on force at break (23.62%) and absorbed energy (20.80%). Most models with P-values above 0.05 are worthless, but a component with a P-value below 0.05 definitely influenced the final model [29,30]. The P-values for the linear coefficients of shape orientation of the re-entrant auxetic structures for force at break and absorbed energy are less than 0.05, as shown in Table 3. However, the cell size of the re-entrant auxetic structure has a P-value lower than 0.05 for force at break and a higher P-value for absorbed energy. As with different porous structures [31], for the re-entrant auxetic structure, shape orientation is an important determinant for both the force at break and energy absorption. Conversely, it may be inferred that the cell size of the re-entrant auxetic structure is more significant for the force at break than for the absorbed energy. This result is consistent with the findings in Figure 7 and Figure 8. Additionally, a numerical technique for model validation has made use of the coefficient of determination R^2 . A high level of agreement between experimental and model findings is indicated by R^2 values near to 1 [32]. Table 3 shows that the model's accuracy is indicated by the R^2 values for force at break (94.49%) and absorbed energy (85.47%).

Table 3. ANOVA for force at break and absorbed energy.

Source	Force at break			Absorbed energy		
	DF	Contribution	P-value	DF	Contribution	P-value
Cell size	2	23.62%	0.036	2	20.80%	0.169
Shape orientation	2	70.88%	0.005	2	64.66%	0.034
Error	4	5.51%		4	14.53%	
Total	8	100%		8	100%	
R^2		94.49%			85.47%	

Figure 9 presents two main effects plots illustrating the impact of cell size and shape orientation on signal-to-noise (S/N) ratios for specific performance metrics. In S/N ratio figures, the highest S/N ratio results in the most optimal levels for running parameters. In subplot (a), the plot shows

S/N ratios for force at break, with distinct trends for each factor. For cell size, the S/N ratio increases as cell size decreases, suggesting that a smaller cell size positively influences the force at break, enhancing the system's robustness to noise. Regarding shape orientation, a significant variation is observed. An orientation of 45° results in a reduction in the S/N ratio, while orientations of 0° and 90° yield higher ratios, with 90° achieving the highest value. This trend implies that aligning shape orientation to 90° could help optimize force at break. Subplot (b) displays the mean values for absorbed energy across the same factor levels. For cell size, the mean absorbed energy increases with smaller cell sizes, mirroring the trend seen for force at break. For shape orientation, the relationship is non-linear. An orientation of 45° leads to notably lower mean absorbed energy, whereas an orientation of 90° yields the highest mean value. This observation is consistent with the literature, demonstrating that shape orientation significantly influences energy absorption capacity [33].

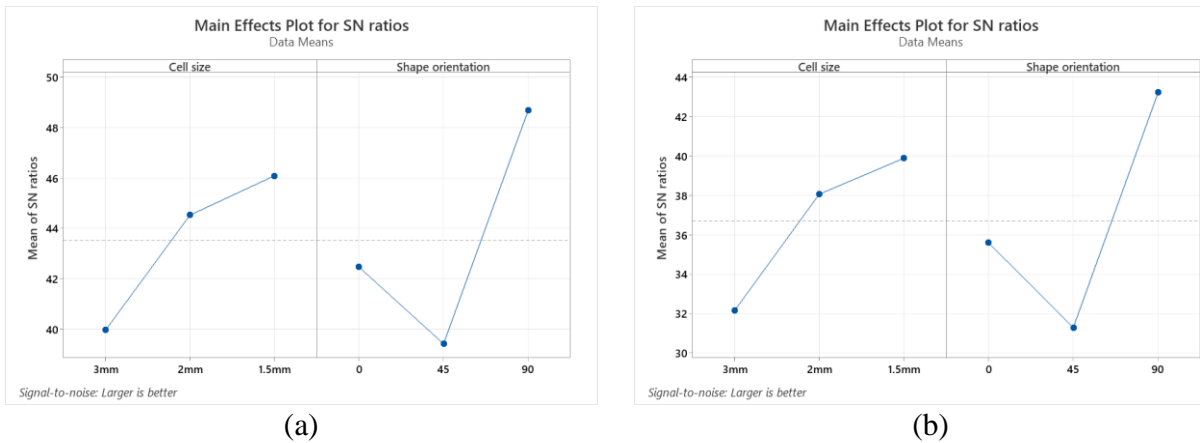


Figure 9. S/N ratios of factor levels for (a) force at break and (b) absorbed energy.

4. CONCLUSIONS (SONUÇLAR)

In this study, tensile mechanical properties of re-entrant auxetic structures produced using different cell sizes and shape orientations were compared with specimens produced in MSLA using commercially available ABS resin. The aim of the research was to determine the cell sizes and shape orientations of re-entrant auxetic structures that provide the highest fracture force and energy absorption. During the production process, configurations with 3 mm, 2 mm and 1.5 mm cell sizes and 0° , 45° and 90° shape orientations were evaluated. The results are summarized in the following:

- 1.5 mm cell size and 90° shape orientation provided the highest fracture force (348.44 N) and energy absorption (224.91 J).
- The lowest fracture force (57.81 N) and energy absorption (17.06 J) were observed in 3 mm cell size and 45° shape orientation.
- Shape orientation had 70.88% and 64.66% effect on fracture force and energy, respectively.
- The effect of cell size on force and energy was lower than shape orientation.

By systematically assessing these features, the development and refinement of engineering systems utilizing auxetic materials for improved performance can be accomplished. Findings in this field can offer significant advantages in the production of aerospace components, medical devices, protective equipment and other devices, especially high energy absorption, adaptability and mechanical robustness.

REFERENCES (KAYNAKLAR)

1. W. Jiang, X. Ren, S.L. Wang, X.G. Zhang, X.Y. Zhang, C. Luo, Y.M. Xie, F. Scarpa, A. Alderson, K.E. Evans, Manufacturing, characteristics and applications of auxetic foams: A state-of-the-art review, *Composites Part B: Engineering*, 235: 109733, 2022.

2. J. Fan, L. Zhang, S. Wei, Z. Zhang, S.-K. Choi, B. Song, Y. Shi, A review of additive manufacturing of metamaterials and developing trends, *Materials Today*, 50: 303–328, 2021.
3. N.K. Choudhry, B. Panda, U.S. Dixit, Energy Absorption Characteristics of Fused Deposition Modeling 3D Printed Auxetic Re-entrant Structures: A Review, *J. of Materi Eng and Perform*, 32: 8981-8999, 2023.
4. O. Duncan, T. Shepherd, C. Moroney, L. Foster, P.D. Venkatraman, K. Winwood, T. Allen, A. Alderson, Review of Auxetic Materials for Sports Applications: Expanding Options in Comfort and Protection, *Applied Sciences*, 8(6): 941, 2018.
5. Y. Kim, K.H. Son, J.W. Lee, Auxetic Structures for Tissue Engineering Scaffolds and Biomedical Devices, *Materials*, 14: 6821, 2021.
6. H. Nguyễn, R. Figueiro, F. Ferreira, Q. Nguyễn. Auxetic Materials and Structures for Potential Defense Applications: An Overview and Recent Developments, *Textile Research Journal*, 93(23-24):5268-5306, 2023.
7. K. Günaydın, O. Gülcan, H.S. Türkmen, Experimental and numerical crushing performance of crash boxes filled with re-entrant and anti-tetrachiral auxetic structures, *International Journal of Crashworthiness*, 28(5) 649-663, 2022.
8. J. Zhang, G. Lu, Z. You, Large deformation and energy absorption of additively manufactured auxetic materials and structures: A review, *Composites Part B: Engineering*, 201: 108340, 2020.
9. A. Joseph, V. Mahesh, D. Harursampath, On the application of additive manufacturing methods for auxetic structures: a review, *Adv. Manuf*, 9: 342-368, 2021.
10. M. Balan P, J. Mertens A, M.V.A.R. Bahubalendruni, Auxetic mechanical metamaterials and their futuristic developments: A state-of-art review, *Materials Today Communications* 34: 105285, 2023.
11. B. Li, W. Liang, L. Zhang, F. Ren, F. Xuan, TPU/CNTs flexible strain sensor with auxetic structure via a novel hybrid manufacturing process of fused deposition modeling 3D printing and ultrasonic cavitation-enabled treatment, *Sensors and Actuators A: Physical*, 340: 113526, 2022.
12. D. Photiou, S. Avraam, F. Sillani, F. Verga, O. Jay, L. Papadakis, Experimental and Numerical Analysis of 3D Printed Polymer Tetra-Petal Auxetic Structures Under Compression, *Applied Sciences*, 11(21): 10362, 2021.
13. S. Shukla, B.K. Behera, R.K. Mishra, M. Tichý, V. Kolář, M. Müller, Modelling of Auxetic Woven Structures for Composite Reinforcement, *Textiles*, 2(1): 1-15, 2022.
14. D. Tahir, M. Zhang, H. Hu, Auxetic Materials for Personal Protection: A Review, *Physica Status Solidi (b)*, 259(12): 2200324, 2022.
15. J.H. Park, H.-J. Park, S.J. Tucker, S.K. Rutledge, L. Wang, M.E. Davis, S.J. Hollister, 3D Printing of Poly- ϵ -Caprolactone (PCL) Auxetic Implants with Advanced Performance for Large Volume Soft Tissue Engineering, *Advanced Functional Materials*, 33(24): 2215220, 2023.
16. Y. Xue, Q. Shao, J. Mu, X. Ji, X. Wang, Compressive Mechanical Behavior of Additively Manufactured 3D Auxetic Metamaterials with Enhanced Strength, *Physica Status Solidi (RRL) – Rapid Research Letters*, 18(2): 2300226, 2024.
17. N.V. Viet, W. Zaki, On exploration of directional extreme mechanical attributes and energy absorption of bending-dominated and buckling-induced negative Poisson's ratio metamaterials, *Composite Structures*, 349-350: 118460, 2024.
18. X. Wu, Y. Su, J. Shi, In-plane impact resistance enhancement with a graded cell-wall angle design for auxetic metamaterials, *Composite Structures*, 247: 112451, 2020.
19. N. Ben Ali, M. Khlif, D. Hammami, C. Bradai, Experimental optimization of process parameters on mechanical properties and the layers adhesion of 3D printed parts, *Journal of Applied Polymer Science*, 139(9): 51706, 2022.
20. A. Temiz, The effect of build orientation on the mechanical properties of a variety of polymer AM-created triply periodic minimal surface structures, *Journal of the Brazilian Society of Mechanical Sciences and Engineering*, 46: 121, 2024.
21. S. Shanmugam, V. Jayaraman, M. Balasubramanian, K. Swaminathan, Optimization of culture parameters for hyper laccase production by *Trichoderma asperellum* by Taguchi design experiment using L-18 orthogonal array, *Malaya Journal of Biosciences*, 1(4): 214-225, 2014.
22. S. Demir, A. Temiz, F. Pehlivan, The investigation of printing parameters effect on tensile characteristics for triply periodic minimal surface designs by Taguchi, *Polymer Engineering & Science*, 64(3): 1209-1221, 2024.

23. F. Pehlivan, Enhancing tensile properties of polymer-based triply periodic minimal surface metamaterial structures: Investigating the impact of post-curing time and layer thickness via response surface methodology, *Polymer Engineering & Science*, 0: 1-14, 2024.
24. A. Temiz, F. Pehlivan, F.H. Öztürk, S. Demir, Compression behavior of sheet-network triply periodic minimal surface metamaterials as a function of density grading, *Journal of Reinforced Plastics and Composites*, 43(23-24): 1430-1443, 2024.
25. F. Pehlivan, F.H. Öztürk, S. Demir, A. Temiz, Optimization of functionally graded solid-network TPMS meta-biomaterials, *Journal of the Mechanical Behavior of Biomedical Materials*, 157: 106609, 2024.
26. L. Yang, O. Harrysson, H. West, D. Cormier, Mechanical properties of 3D re-entrant honeycomb auxetic structures realized via additive manufacturing, *International Journal of Solids and Structures*, 69-70: 475-490, 2015.
27. J. Shen, K. Liu, Q. Zeng, J. Ge, Z. Dong, J. Liang, Design and mechanical property studies of 3D re-entrant lattice auxetic structure, *Aerospace Science and Technology*, 118: 106998, 2021.
28. H. Khan, M. ur R. Siddiqi, S. Saher, R. Muhammad, M.S. Rehan, Tensile properties of 3D-printed PLA prismatic cellular structures: an experimental investigation, *Int J Adv Manuf Technol*, 134: 4399-4410, 2024.
29. F.H. Öztürk, Optimization of adherend thickness and overlap length on failure load of bonded 3D printed PETG parts using response surface method, *Rapid Prototyping Journal*, 30(8): 1579-1591, 2024.
30. S. Simsek, S. Uslu, Determination of a diesel engine operating parameters powered with canola, safflower and waste vegetable oil based biodiesel combination using response surface methodology (RSM), *Fuel*, 270: 117496, 2020.
31. P. Wang, Y. Bian, F. Yang, H. Fan, B. Zheng, Mechanical properties and energy absorption of FCC lattice structures with different orientation angles, *Acta Mech*, 231: 3129-3144, 2020.
32. A. Temiz, The Effects of Process Parameters on Tensile Characteristics and Printing Time for Masked Stereolithography Components, Analyzed Using the Response Surface Method, *J. of Materi Eng and Perform*, 33: 9356–9365, 2024.
33. M. Xu, Z. Xu, Z. Zhang, H. Lei, Y. Bai, D. Fang, Mechanical properties and energy absorption capability of AuxHex structure under in-plane compression: Theoretical and experimental studies, *International Journal of Mechanical Sciences*, 159: 43-57, 2019.